Surface Science 143 (1984) 495–508
North-Holland, Amsterdam

DIRECT ATOMIC IMAGING OF SOLID SURFACES
II. Gold (111) surfaces during and after in situ carbon etching

L.D. MARKS *

Department of Physics, Madingley Road, Cambridge CB3 OHE, UK

and

David J. SMITH

High Resolution Electron Microscope, University of Cambridge, Free School Lane, Cambridge CB2 3RQ, UK

Received 6 January 1984; accepted for publication 16 March 1984

High resolution electron micrographs are presented which show the atomic structure of gold (111) surfaces during and after electron-beam-induced etching of surface carbon contaminants by water vapour. Initial carbon removal leaves a persistent electron-beam-resistant layer on the surface which is believed to be molecular benzene with a Van der Waals spacing of 7.3 Å. During this removal process and later cleaning, elastic deformations of the gold indicated by large, normal surface expansions (typically ~10%) and the development of a pronounced "hill and valley" morphology are observed. Accommodation of these elastic deformations by surface dislocations is also observed. These point to an in-plane expansion on the gold (111) surface which is estimated at 5%. Finally, the results are related to a recent solid state model for gold surfaces, experimental observations on multiply twinned particles and stacking faults in small gold particles, and the occurrence of benzene is linked to the mechanism of the etching process.

1. Introduction

Obtaining detailed information about surface structures on the atomic scale in real space, thereby avoiding the averaging problems inherent in diffraction methods, has been a goal of electron microscopists for many years. Considerable progress has recently been achieved using dark field techniques in ultra-high vacuum, but with the somewhat limited resolution of about 1 nm (for a recent review see ref. [1]). At this level of detail, however, it is impossible to obtain information about specific atom site locations, although extensive other information about surfaces, including reconstructions, is available.

* Now at Physics Department, Arizona State University, Tempe, Arizona 85287, USA.

0039-6028/84/$03.00 © Elsevier Science Publishers B.V.
(North-Holland Physics Publishing Division)

In recent axial bright-field observations we have demonstrated that high resolution imaging of specimens in a surface projection orientation can reveal directly the atomic surface structure [2], including the facetting and the presence and nature of any surface reconstructions [2–4]. For example, we have confirmed [2] the missing row model [5] for the 2×1 gold (110) surface, and measured a 20% ($\pm 5\%$) outer atom expansion on this surface together with a 10% ($\pm 5\%$) outer atom expansion on local areas of clean 1×1 surfaces [4]. These latter results were for the surfaces of small gold particles cleaned by in situ etching of the carbon support film, and the detailed interpretation of the experimental images was by synergistic experiment and numerical calculation, details of which have been previously described [6].

In this paper we present detailed observation of extended gold (111) surfaces during and after the removal of carbon contaminants by electron-beam-induced water etching. It should be appreciated that the experimental micrographs represent two-dimensional projections of what appears to be an intrinsically rough three-dimensional surface. This effectively makes it not feasible to carry out a thorough analysis using image simulations, in contrast to the gold (110) surface [4] where quantitative measurement of surface relaxations was possible. Thus, although the expansive trends of the surface during the observations could be reliably identified, quantitative evaluation has been deliberately avoided.

The basic outline of the experimental parts (section 3) of the paper follows the time evolution of the gold (111) surfaces, with section 3.1 describing the initial carbon removal procedure and the development of a hill and valley structure. The occurrence of a molecular layer believed to be benzene on the gold surface after removal of most of an initial carbonaceous contamination layer is then described (section 3.2). Following this, a number of structural effects, all of which correlate with in-plane surface expansions, are presented and elastic (i.e. relaxations) and plastic effects (surface dislocations) are described (section 3.3). Finally, it is shown that these various phenomena correlate with the behaviour of clean gold surfaces predicted from a recent theoretical model (section 4, 5 and refs. [7,8]), and some morphological phenomena in small gold particles (section 5). Some preliminary results of this study have been reported elsewhere [8] and a general account of our observations of small metal particles and extended Au surfaces will also be described elsewhere [9].

2. Experimental methods

2.1. Sample preparation

Two types of specimens were employed in this study, namely small particles supported on amorphous carbon prepared in the manner described elsewhere

[2], and (100) epitaxial holey gold films of 10–20 nm thickness. The latter appear highly promising as viable specimens for studies of the surface structure of gold and other materials and were prepared in the following manner.

Gold was evaporated in an *unbaked* UHV evaporator onto in situ cleaved KCl at 270°C at a pressure of $\sim 2 \times 10^{-6}$ Torr, soon after loading a fresh KCl substrate into the system. Under these conditions the dominant residual contaminant (determined by mass spectrometry) was water, with traces of carbon monoxide and nitrogen *. The semi-continuous films were then annealed for at least a day in situ at 270°C to promote grain growth and to remove most of the residual strains. The gold films were then transferred (very gently) by flotation in a 1 : 4 ethanol/water mix onto holey carbon films ready for observations in the electron microscope.

2.2. Imaging methods

The specimens were examined in the Cambridge University High Resolution Electron Microscope [14] operated at 500 kV, typical operating conditions being an electron-optical magnification of 8×10^5, a convergence semi-angle of 0.5 mRad and a focal spread of ~ 16 nm. The typical current density at the sample was about 20 A/cm^2 ($\sim 10^4$ e$^-$ per second per Å^2). Image interpretations were confirmed by comparing digital microdensitometry of the photographic negatives with theoretical image simulations: details have been described elsewhere [6].

2.3. In situ cleaning

As prepared, the holey gold films were covered in approximately 5 nm of carbonaceous material, probably arising from atmospheric pollution during transfer of the specimen. In situ removal of the carbon was due to residual water vapour in the microscope vacuum, initially from freshly introduced photographic films which had not been fully desiccated. More controlled etching (albeit somewhat slower) resulted from a deliberate moist air leak. We have subsequently been able to remove the carbonaceous layer in a UHV scanning transmission electron microscope with a residual gas pressure of about 10^{-7} Torr of water (measured by mass spectrometry) and some high molecular weight hydrocarbon residues. This confirmed that water was the active agent. Also note that carbon etching in an electron microscope is a well-known phenomenon (e.g. ref. [15]).

Although the residual vacuum was comparatively poor in ultra-high-vacuum

* For reasons that are not properly understood, water contamination strongly favours the formation of (100) square pyramid nuclei, rather than multiply-twinned particles [10–13], assisting in the formation of a low defect (100) film.

terms ($\sim 5 \times 10^{-7}$ Torr), once the surface contaminants were removed a clean surface was retained. Gold is chemically inert so that physisorption of almost all species should be prevented by the high electron flux, both primary and secondary, with radiation damage, both ionisation and knock-on (e.g. ref. [16]) desorbing most weakly adsorbed species. We note that electron beam heating should be minimal with a good thermal conductor such as gold or amorphous carbon, and that there was no evidence for surface roughening on other gold surfaces such as (100), ruling out the possibility of artifacts from ion or electron beam damage of the gold. Furthermore, surface species can be clearly imaged when present [6], so we could monitor the surface cleanliness in situ. This film preparation technique may be viable for silver surfaces, but will probably not succeed for more reactive metals such as platinum: cleaner vacuums will be required together with other gas phase cleaning procedures (e.g. hydrogen to remove any surface oxide).

3. Results

The holey gold films consisted of continuous films with many crystallographic holes of various shapes and sizes, as shown in fig. 1. Many different surfaces are thus made available in the projection orientation required for atomic level surface imaging: in this paper only (111) facets viewed down a (110) axis are described. For convenience, the results are divided into three sections, corresponding to the dominant surface structures observed.

3.1. Initial carbon etching – development of hill and valley structures

The most distinctive and somewhat surprising feature observed was the transformation from relatively flat (111) facets to a pronounced hill and valley

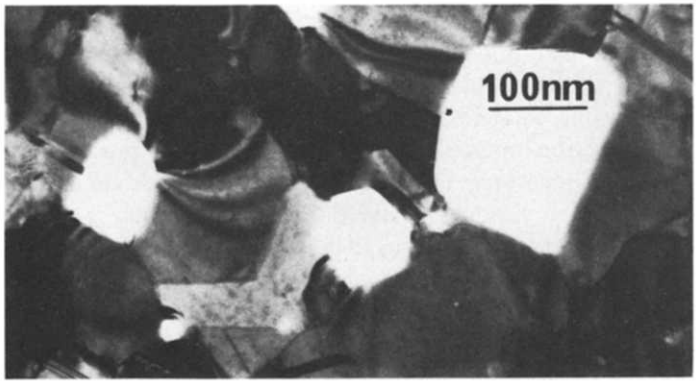

Fig. 1. Low magnification image showing the typical morphology of the semi-continuous, holey Au films.

structure as shown in fig. 2. This morphology gradually developed on the holey gold films as the carbon was etched away, with hill heights typically reaching five or six atomic layers. On the small metal particles a slightly different structure was observed to occur (fig. 3) which could be described as a long

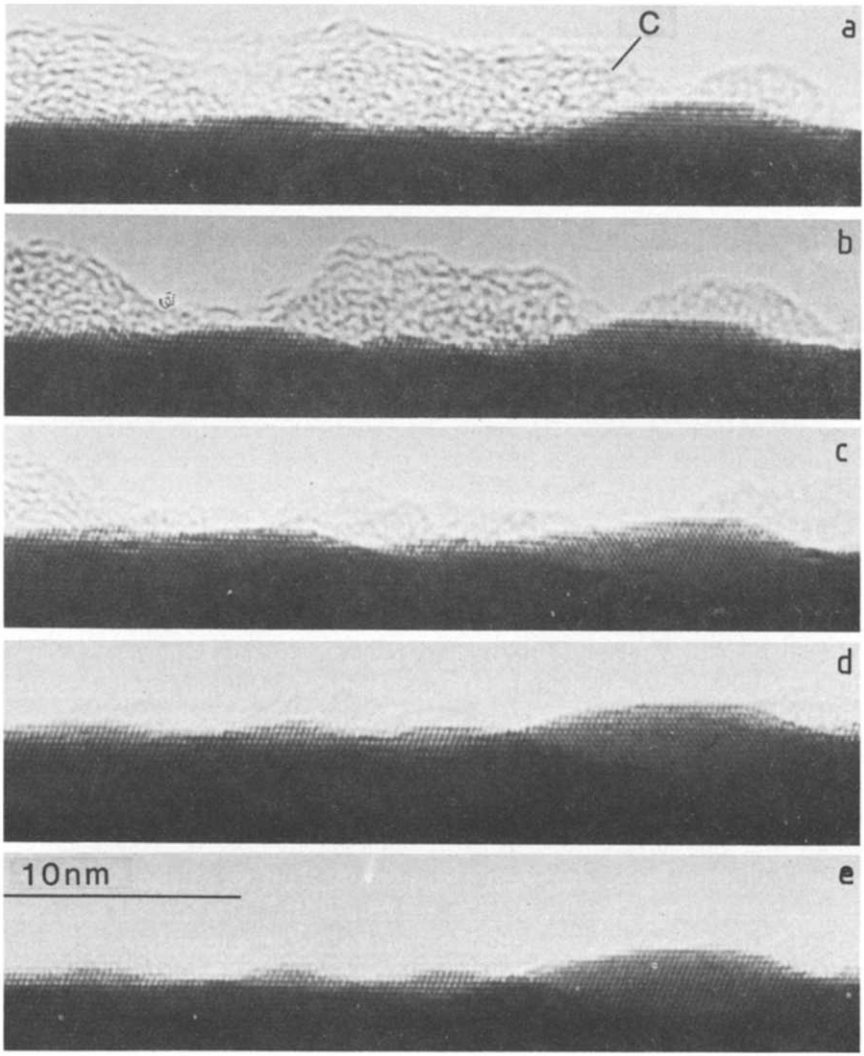

Fig. 2. Series of high-resolution images of a (110)-projection (111) surface, recorded over a period of about 20 min, showing the etching away of the carbonaceous surface overlayer and the development of a pronounced three-dimensional hill-and-valley surface structure. The typical "speckle" pattern of amorphous carbon is indicated.

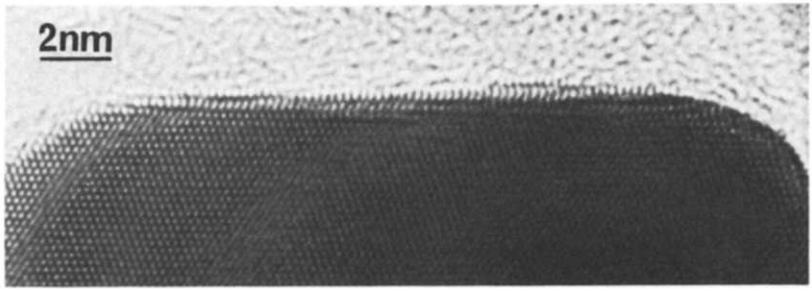

Fig. 3. Surface structure of a square-pyramidal particle of gold showing evidence for surface distortion. The background is partially etched amorphous carbon.

range buckle distortion. Both these morphologies can be explained in terms of an in-plane surface expansion with different boundary conditions (see section 4).

The carbon etching reaction proceeded somewhat inhomogeneously, suggesting that several different mechanisms were occurring simultaneously (see fig. 2). There appeared to be non-localised etching over the whole carbon film (evidenced by loss in contrast), some suggestion of preferential etching on (100) surfaces (here, (100) sides of the hills) and tearing along the surface.

3.2. Persistent surface layers – a benzene superstructure

When most of the carbonaceous material had been removed, surface structures such as that shown in fig. 4 generally remained. These surface layers proved surprisingly resistant to the etching process, typically requiring as long again to remove from the gold surface as did the bulk of the original amorphous layer (i.e. 30 min or more).

The crucial information required for detailed interpretation of this structure is the noticeably different image contrast at the two defoci shown in figs. 4a and 4b. In fig. 4a the image contrast is black at the positions of the gold atomic columns, and the surface superstructure shows a number of "black dots" suggesting atomic columns. By comparison, at the defocus where the gold column positions in the bulk of the specimen appear white (fig. 4b), the surface superstructure is imaged with very low contrast. Note that the spacings present are complicated, as shown in fig. 4c. The image simulations in fig. 5 indicate that, whereas the "black dot" contrast of fig. 4a could be interpreted in terms of either a gold *or* carbon superstructure laterally expanded by about 20% relative to the bulk, at the defocus corresponding to the bulk "white dot" contrast only a carbon surface layer is imaged with very low contrast, corresponding to the experimental images.

A simple hexagonal carbon superstructure as used in the simulations for fig.

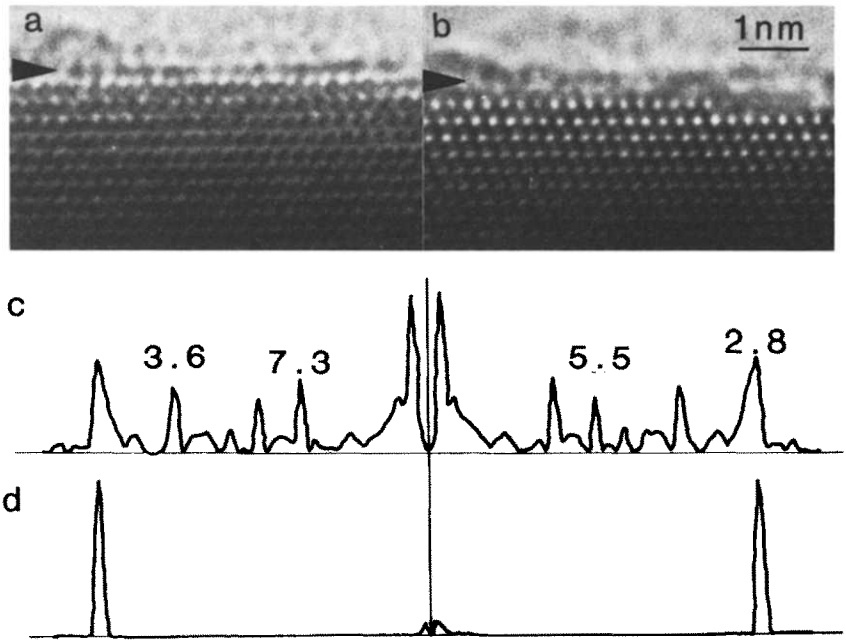

Fig. 4. Pair of high-resolution images recorded at (a) optimum defocus (black Au atom columns) and (b) reverse contrast (white Au atom columns). A power spectra taken through the surface layer is shown in (c) with the main spacings marked and in (d) from the bulk. In (b), the carbonaceous surface layer (arrowed) is imaged with very low contrast, thereby enabling the Au atom columns to be identified. Further details of the imaging effects can be found in ref. [6].

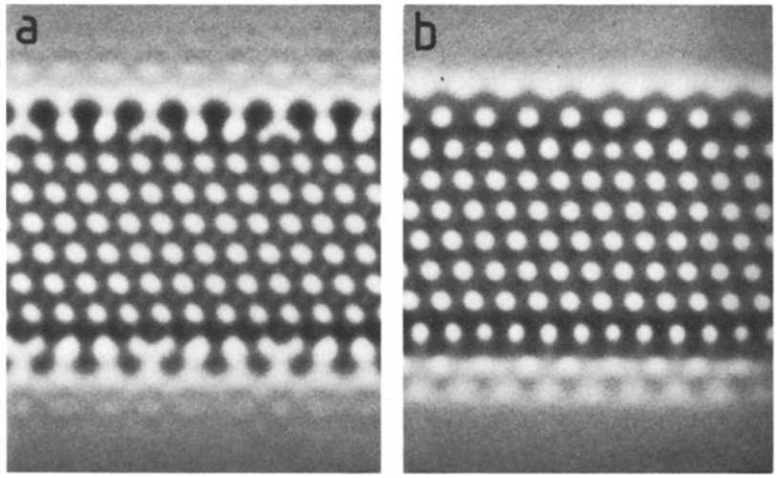

Fig. 5. Image simulation showing gold crystal with surface layers of gold (top) and carbon (bottom) expanded by ~ 20% relative to the bulk. At optimum defocus (a), both surface layers are imaged with high contrast but, at the reverse "white dot" defocus (b), only the gold layer has high contrast. The carbon contrast qualitatively follows the experimental results.

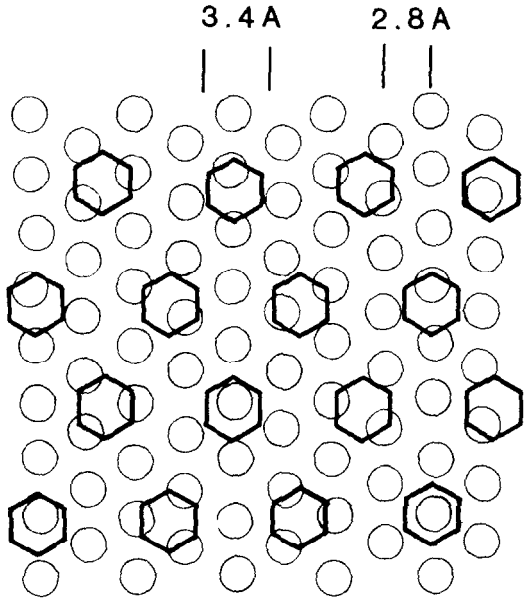

Fig. 6. Schematic model in normal view of a hexagonal layer of benzene molecules on the gold (111) surface, corresponding to a Van der Waals surface layer.

5 is, however, chemically unrealistic; the carbon–carbon bond distance is about 3.4 Å, with a carbon–surface separation of about 2.5 Å, and both of these values are unreasonably large. It is significant to note here that aromatic or graphitic contaminants have been observed on small silver or gold particles

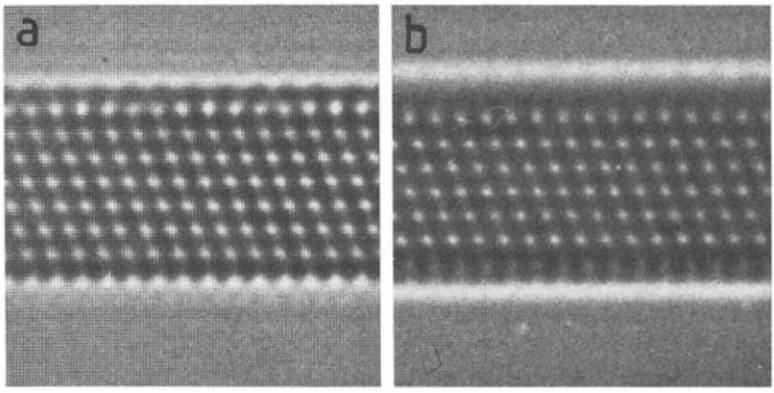

Fig. 7. Image simulation of projected Au(111) surface having a benzene surface layer (at top) corresponding to model shown in fig. 6. (a) Optimum defocus of −600 Å; (b) "white dot" defocus of −900 Å. See also ref. [6].

(prepared and examined in UHV without deliberate contamination) using surface-enhanced Raman scattering [17]. Furthermore, aromatic or graphitic species epitaxial on (111) fcc surfaces are relatively well known (e.g. ref. [18]). Therefore, we may expect some form of hydrocarbon and, indeed, a simple model of a hexagonal layer of benzene molecules on the gold (111) surface separated by the Van der Waals radii (see fig. 6) is an excellent fit to the observed contrast and spacings as shown by the image simulations in fig. 7. The digital power spectrum in fig. 4c is the most accurate measurement of the surface spacings, showing a 7.3 Å benzene lattice spacing, the 3.6 Å half spacing and a 5.3 Å moiré spacing. We note that other carbonaceous layers such as a graphitic superstructure or gold containing compounds were exceedingly bad fits to the experimental results; graphite would show a strong black line for the defocus of fig. 4a, whilst gold structures would show contrast for the defocus of fig. 4b.

3.3. Clean surfaces

Following removal of the benzene superstructure, the surface typically exhibited a buckled and distorted morphology as shown in figs. 8a and 8b. By

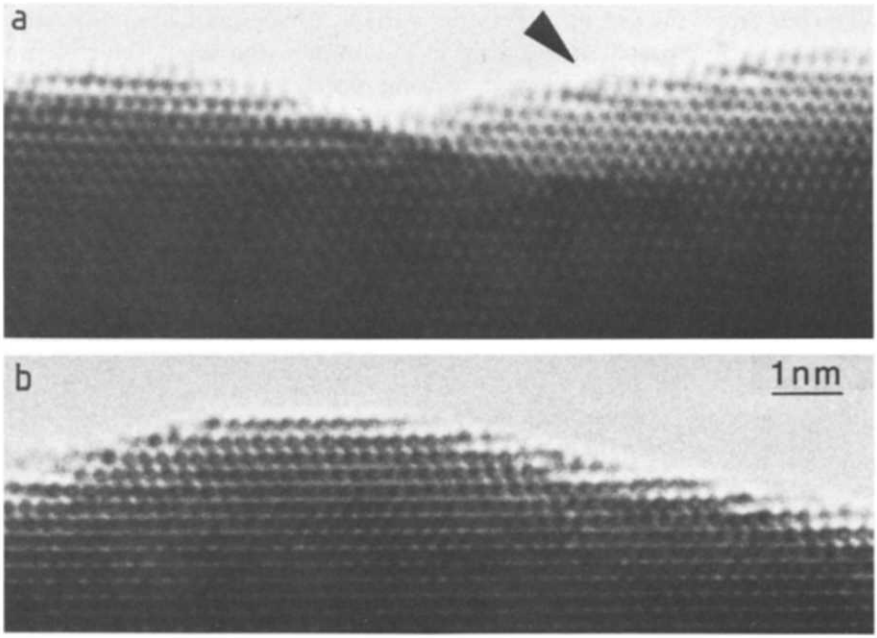

Fig. 8. Images showing development of "hill-and-valley" surface after removal of benzene superstructure. Note large expansive distortions of the surface layers (arrowed), best observed by viewing along the line of the fringes.

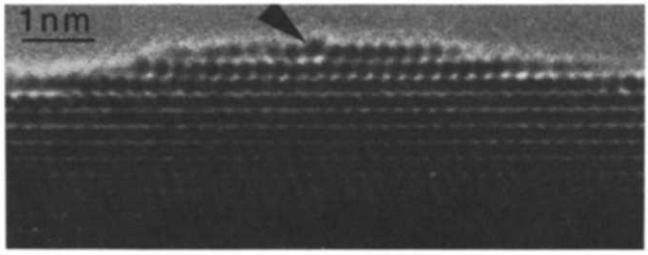

Fig. 9. High-resolution image of Au surface showing a prominent lattice defect (arrowed) identified as a surface partial dislocation since it separates a region of BABC stacking from one of BABA stacking.

this stage no surface carbon appeared to remain (except for a few isolated clumps), as confirmed by the characteristic appearance with lens defocus described in section 3.2. Large distortions (~ 15% of the interplanar spacings, as measured digitally) were evident at the tops of the hills and in the region of steps (fig. 8), always in an expansive sense. Image simulations showed that from the microscope used herein, the actual outwards expansion was approximately 5% less than the apparent expansion in the images [6]. This 5% shift arises from Fresnel effects at the surface. However, the caveat with respect to overinterpretation described in the introduction should be remembered. Other structural features were stacking mistakes (stacking faults) in the surface layer, as well as surface partial dislocations, as shown in fig. 9. (These occurred less frequently for the benzene covered surface of section 3.2.) Most of these dislocations were identified as being of Shockley partial nature and were always found to be of vacancy rather than interstitial type (with one less column of atoms rather than one more), i.e. a standard, bulk Shockley partial "cut" by the (111) surface plane.

Eventually, the structure evolved to a relatively well-ordered surface with smaller distortions as shown in fig. 10. This process was observed by an image

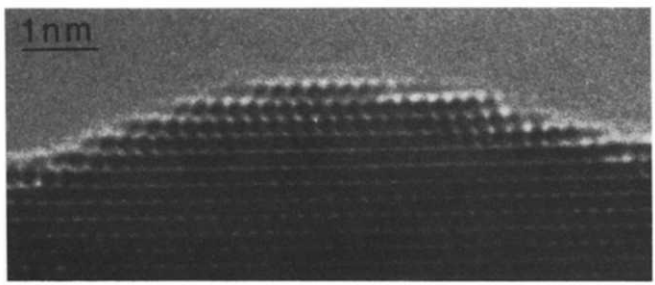

Fig. 10. Relatively well-ordered surface with small (~ 5%) expansions at the surface steps.

pick-up and viewing system [19] to be due to surface diffusion. There were still expansions of about 5%, primarily at the surface steps and on the (110) sides of the hills. These (110) expansions correspond very well with the expansions of (110) 1×1 and 2×1 surfaces which have been described elsewhere [4].

4. Surface expansions on gold (111)

In this section the observations presented in section 3 are correlated with earlier work on gold (110) surfaces [4] and explained in terms of in-plane expansions.

The first results to consider are the hill and valley structure for the holey gold films (fig. 2) and the surface buckle for the discrete particles (fig. 3). It is relevant that the surfaces in the holey gold films are at holes ($\sim$ 50 nm in radius, see fig. 1) in the film, so that there is little space available for a flat surface to expand laterally. In contrast, no such constraint acts on a discrete particle ($\sim$ 10 nm radius) and an expansive buckle can readily occur on a flat surface. The hill and valley morphology can thus be rationalised in terms of providing space for the sideways expansion.

Clear evidence for these expansions is evident from the disordered surfaces shown in section 3.3, for example fig. 8. We note the very strong similarity between the experimental images and early calculations of surfaces and surface step configurations, e.g. ref. [20]. These calculations used somewhat simplified pair-wise potentials without a (more realistic) oscillatory tail, but contain an intrinsic expansive tangential surface pressure. The noticeable expansion of the top layer corresponds to a normal displacement induced by a tangential surface pressure with a constraint for the atoms to sit in-register on the lattice below. The distortions to the lower layers around the steps are due to the back-pressure of the outermost layer. We also note that expansions of about 10% ($\pm$5%) occur in the atom positions at the steps which are locally (110). This agrees with the 10% expansion observed for clean gold (110) surfaces. Indeed, following a model for the (110) reconstruction as a surface decomposition into (110) facets (21) the experimental 20% expansion on the 2×1 (110) surface [4] can be considered as accommodating the in-plane (111) expansion, the (110) and (111) results both being consistent with a 5% (111) expansion.

The final surface (section 3.3) still displays some expansion, but there are now more stacking faults and surface partial dislocations – the elastic distortions have nucleated plastic defects to accommodate the surface expansion.

We note that our interpretation of the hill-and-valley structure is as a manifestation of an expansive tangential surface pressure – the well-annealed surface will probably contain a dislocation array to accommodate the pressure, and be flat.

5. Discussion

In the preceding sections we have described the changes of morphology observed on gold (111) surfaces during and following removal of carbon by electron-beam-induced water etching. There is extensive semi-quantitative evidence for in-plane expansions which, for the constrained holey gold films, are accommodated first by a hill and valley structure (or a buckle on the small particles), and eventually by plastic deformation involving surface dislocations. For completeness, we should emphasise that the expansions only occur when the carbon is absent which was the behaviour previously observed for gold (110) surfaces [4]. Finally, it should be noted that the elastic deformations were not confined solely to the outermost surface layer – strain contrast effects were often observed below the surface (e.g. fig. 3).

It is relevant to point out the existence of a theoretical model for the expansions which will be described in detail elsewhere [7,8]. In a transition metal the bonding between atoms can be considered as a balance between a pair-wise pseudopotential from the d electrons, and a nearly free electron (NFE) term from the s and p electrons. The bulk interatomic spacing can be considered as resulting from a balance between a pseudopotential and a NFE pressure, and for gold the NFE is attractive whilst the pseudopotential is repulsive [22–25]. At a clean surface, the NFE electrons retract into the bulk for gold leaving a repulsive pseudopotential. This leads to a tangential surface pressure driving the experimentally observed expansions. A carbon covering could stabilise the surface cancelling out the expansive pressure.

The occurrence of a molecular benzene superstructure provides some key information to the cleaning mechanism. It is reasonable to assume that the water–gas reaction takes place, the main products being carbon monoxide and hydrocarbons. The initial (rate limiting) step must involve an electron beam activated process, probably a carbon bond fission or a π to π^* transition. Carbon monoxide will be produced and released, with the amorphous carbon acting as a sink for the hydrogen. Further skeletal rearrangements can take place in the hydrocarbon layer, probably typical cracking reactions. Benzene can be produced, and, being a relatively unreactive compound, remain for a substantial time on the surface. Further studies using high energy electrons in a conventional UHV surface science instrument would be of interest.

One problem with the existence of carbonaceous superstructures on gold (111) is that some doubt must be cast on the validity of the 22×1 reconstruction [1,26–29]. Auger detection of carbon on silver and gold is not straightforward; the carbon Auger signal overlaps with a strong, secondary peak from the metal. In order to detect by Auger a monolayer carbon coverage, it is necessary to very carefully subtract the bulk metal signal [30], and its presence in the raw data is not obvious [30]. UHV prepared silver and gold particles almost invariably show evidence for some carbonaceous contaminants in surface

enhanced Raman scattering [17], which are very difficult to remove even with an ion beam [17] or detect by Auger.

Hence there would appear to be good circumstantial evidence for possible carbonaceous contaminants on the "known" 22×1 reconstruction [26–29]. The evidence for this reconstruction is a spacing at 1.4 Å, which is still present after extensive, rough handling including exposure to a plastic and air [29]. Unfortunately, a 1.4 Å spacing is exactly what would be expected from a carbon double bond. Consequently the presence of undetected carbon is a possible explanation of the apparent earlier reports of a surface contraction, opposite to our results of an expansion.

One could perhaps argue that our results have been modified by (undetected) lattice hydrogen, but this would appear to be a little unreasonable. We have linked the (111) expansion with the (110) surface expansion [4], following the model of Binnig and Rohrer [21] of the (110) surface decomposing into (111) microfacets. Hence the fact that the expansion on (110) surfaces has also been detected by X-ray [31] and ion scattering experiments [32] would appear to rule out hydrogen effects.

Finally, we should point out the strong connection of our results with other experimental observations for gold, namely the common occurrence of multiply-twinned particles (e.g. refs. [10–13]) and stacking faults in small particles (e.g. refs. [33,34]). It has recently been shown that an expansive tangential surface presure will strongly favour the formation of multiply-twinned particles [12,13]. These are very common for gold and silver, substantially less so for other metals. In addition, one of the earliest models for these stacking faults was in terms of surface stacking mistakes [33], and the model for the gold (111) reconstruction described herein leads naturally to many stacking mistakes. These correlations demonstrate the perhaps unsurprising fact that surface phenomena such as reconstructions are very important in understanding the morphology and growth of small metal particles. This supports the view that surface phenomena studied in high vacuum conditions are relevant to heterogeneous catalysis by small metal particles.

Acknowledgments

This work has been supported by the Science and Engineering Research Council, UK. We are grateful to Dr. A Howie and Professor V. Heine for their useful comments on parts of this work.

References

[1] K. Takayanagi and K. Yagi, Trans. Japan Inst. Metals 24 (1983) 337.
[2] L.D. Marks and D.J. Smith, Nature 303 (1983) 315.

[3] D.J. Smith and L.D. Marks, in: Proc. 7th Intern. Conf. on High Voltage Electron Microscopy, Lawrence Berkeley Laboratory, Berkeley, CA, 1983, Eds. R.M. Fisher, R. Gronsky and K.H. Westmacott, pp. 53–58.
[4] L.D. Marks, Phys. Rev. Letters 51 (1983) 1000.
[5] H.P. Bonzel and S. Ferrer, Surface Sci. 118 (1982) L263.
[6] L.D. Marks, Surface Sci. 139 (1984) 281.
[7] L.D. Marks, V. Heine and D.J. Smith, Phys. Rev. Letters 52 (1984) 656.
[8] V. Heine and L.D. Marks, in preparation.
[9] D.J. Smith and L.D. Marks, in preparation.
[10] S. Ino, J. Phys. Soc. Japan 21 (1966) 346.
[11] S. Ino and T. Ogawa, J. Phys. Soc. Japan 22 (1967) 1369.
[12] L.D. Marks, Phil. Mag. A49 (1984) 81.
[13] A. Howie and L.D. Marks, Phil. Mag. A49 (1984) 95.
[14] D.J. Smith, R.A. Camps, V.E. Cosslett, L.A. Freeman, W.O. Saxton, W.C. Nixon, H. Ahmed, C.J.D. Catto, J.R.A. Cleaver, K.C.A. Smith and A.E. Timbs, Ultramicroscopy 9 (1982) 203.
[15] H.G. Heide, in: Proc. 5th Intern. Conf. on Electron Microscopy, Vol. 1, Ed. S.S. Breese, Jr. (Academic Press, New York, 1962) pp. A4–A5.
[16] R.M. Glaeser and K.A. Taylor, J. Microscopy 112 (1978) 127, who described damage to biological specimens which is probably similar.
[17] C.E. Murray, private communication.
[18] S.R. Keleman and T.E. Fischer, Surface Sci. 102 (1981) 45.
[19] C.J.D. Catto, K.C.A. Smith, W.C. Nixon, S.J. Erasmus and D.J. Smith, Inst. Phys. Conf. Ser. 61 (1982) 123.
[20] P. Wynblatt, in: Interatomic Potentials and Simulation of Lattice Defects Eds. Gehlen, Beeler and Jaffee (Plenum, New York, 1972) p. 633.
[21] G. Binnig and H. Rohrer, personal communication.
[22] V. Heine, Solid State Phys. 35 (1980) 1, especially pp. 111–114.
[23] M.V. Nevitt, and subsequent discussion, in: Phase Stability of Metals and Alloys, Eds. Rudman, Stringer and Jaffe (McGraw-Hill, New York, 1967) p. 281.
[24] D.G. Pettifor, J. Phys. F (Met. Phys.) 8 (1978) 219.
[25] N.E. Christiansen, private communication.
[26] J. Perdereau, J.P. Biberian and G.E. Rhead, J. Phys. F4 (1978) 798.
[27] H. Mele and E. Menzel, Z. Naturforsch. 33a (1978) 282.
[28] Y. Tanishiro, H. Kanamori, K. Takayanagi, K. Yagi and G. Honjo, Surface Sci. 111 (1981) 395.
[29] J.C. Heyraud and J.J. Métois, Surface Sci. 100 (1980) 519.
[30] Gold has a similar Auger spectrum to silver, which is discussed by S.R. Keleman and I.E. Wachs, Surface Sci. 97 (1980) L370.
[31] I.K. Robinson, Phys. Rev. Letters 50 (1983) 265.
[32] R.J. Culbertson, private communication.
[33] M.J. Hall and M.W. Thompson, Brit. J. Appl. Phys. 12 (1961) 495.
[34] J.W. Matthews and D.L. Allinson, Phil. Mag. 8 (1963) 1283.